

SUPPORTING INFORMATION

High performing PbS Quantum Dot Sensitized Solar Cells exceeding 4% efficiency: The role of metal precursor in the electron injection and charge separation

Victoria González-Pedro,¹ Cornelia Sima,^{1,2,3} Gabriela Marzari,¹ Pablo P. Boix,¹ Sixto Giménez,¹ Qing Shen,^{4,5} Thomas Dittrich,⁶ and Iván Mora-Seró*¹

¹ Photovoltaic and Optoelectronic Devices Group, Departament de Física, Universitat Jaume I, 12071 Castelló, Spain.

² University of Bucharest, Faculty of Physics, 405 Atomistilor, P.O. Box MG-11, 077125, Bucharest-Magurele, Romania

³ National Institute of Lasers, Plasma and Radiation Physics, Atomistilor 409 street, P.O. Box MG 36 Bucharest-Magurele, 077125, Romania.

⁴ Department of Engineering Science, Faculty of Informatics and Engineering, The University of Electro-Communications, 1-5-1 Chofugaoka, Chofu, Tokyo 182-8585, Japan.

⁵ PRESTO, Japan Science and Technology Agency (JST), 4-1-8 Honcho, Kawaguchi, Saitama 332-0012, Japan.

⁶ Helmholtz-Zentrum Berlin für Materialien und Energie GmbH, Glienicker Strasse 100, 14109 Berlin, Germany.

*Corresponding authors: sero@fca.uji.es

SI.1.- Transmission Electron Microscopy (TEM) characterization:

(a)

(b)

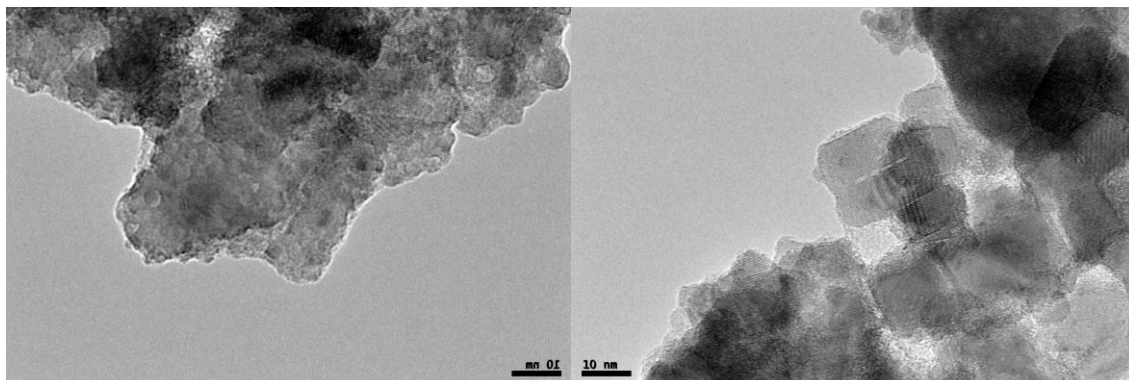


Figure S.1. Transmission Electron Microscopy (TEM) images of nanoporous TiO_2 films covered with PbS/CdS QDs (2 and 5 SILAR cycles for PbS and CdS deposition, respectively). Lead precursors were (a) acetate and (b) nitrate salts.

SI.2.- Reproducibility of Solar Cell Performance:

Study of cell reproducibility. The films were sensitized by SILAR using 2 SILAR cycles PbS plus 5 cycles CdS and different lead precursor, acetate (Ac) and nitrate (N). The efficiency of (Ac)/(Ac) and (N)/(Ac) from the average value and the standard error of the average value are: $3.89 \pm 0.24\%$ and $3.62 \pm 0.15\%$ respectively. The dispersion in (Ac)/(Ac) and (N)/(Ac) samples considering the relative error is 6% and 4% respectively.

Sample (PbS/CdS)	J_{sc} (mA/cm^2)	V_{oc} (V)	FF	η (%)
(Ac)/(Ac)	22.28	0.416	0.453	4.20
	21.08	0.432	0.424	3.86
	20.16	0.416	0.451	3.78
	21.32	0.422	0.393	3.53
	18.88	0.474	0.458	4.10
(N)/(Ac)	18.98	0.485	0.415	3.82
	15.05	0.412	0.548	3.40
	13.46	0.443	0.601	3.62
	16.25	0.478	0.452	3.51
	14.22	0.446	0.593	3.76

SI.3.- Dependence of cell performance on CdS SILAR cycles and on cadmium precursor:

Photovoltaic parameters for co-sensitized PbS/CdS and single sensitized CdS cell devices varying de cadmium source (acetate, Ac, and nitrate, N) and the number of SILAR cycles. PbS deposition was fixed in 2 SILAR cycles.

Sample (PbS/CdS)	N° SILAR cycles (PbS/CdS)	J_{sc} (mA/cm ²)	V_{oc} (V)	FF	η (%)
(Ac)/(Ac)	2/5	22.28	0.416	0.453	4.20
(Ac)/(N)	2/5	10.24	0.318	0.512	1.72
(Ac)/(N)	2/10	16.43	0.475	0.426	3.33
CdS(A)	0/5	9.54	0.566	0.524	2.83
CdS (N)	0/10	7.56	0.547	0.526	2.17

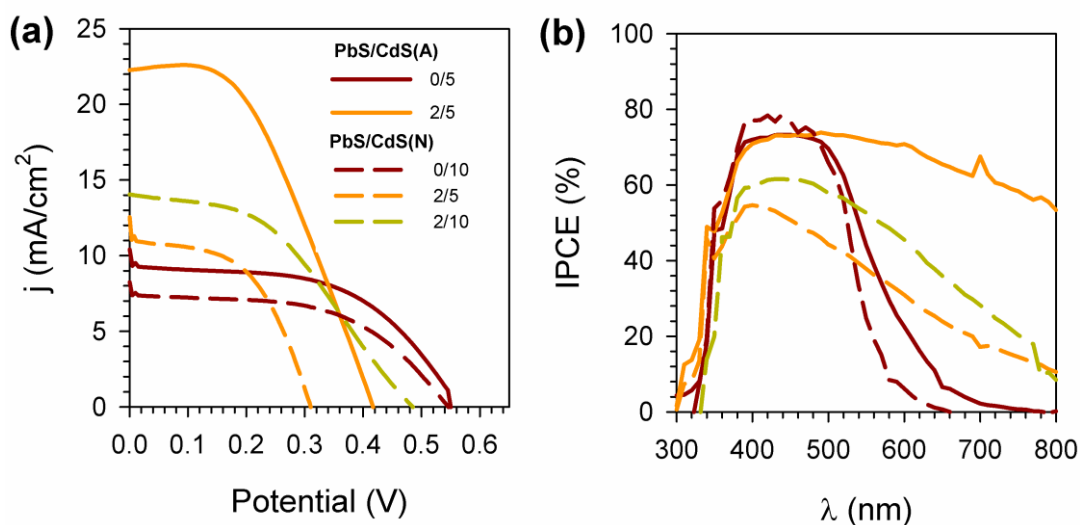


Fig.SI.3. (a) Current-Voltage curves, and (b) IPCE for co-sensitized PbS/CdS and single sensitized CdS cells varying the number of CdS cycles and the cadmium precursor, acetate (solid line) and nitrate (dashed line). PbS deposition was fixed in 2 SILAR cycles and the Pb precursor was lead acetate in all the cases. The presence of PbS extend the light absorption to longer wavelengths. The kind of cadmium precursor used for CdS grown has a dramatic effect on solar cell performance, especially on the photocurrent. The notation (X/Y) is referred to the number of SILAR cycles for PbS (X) and CdS (Y), respectively. Samples PbS/CdS (A) (0./5) and PbS(N)/ CdS (0/10) are films with similar absorption proprieties and comparable on the basis of photocarriers generated.

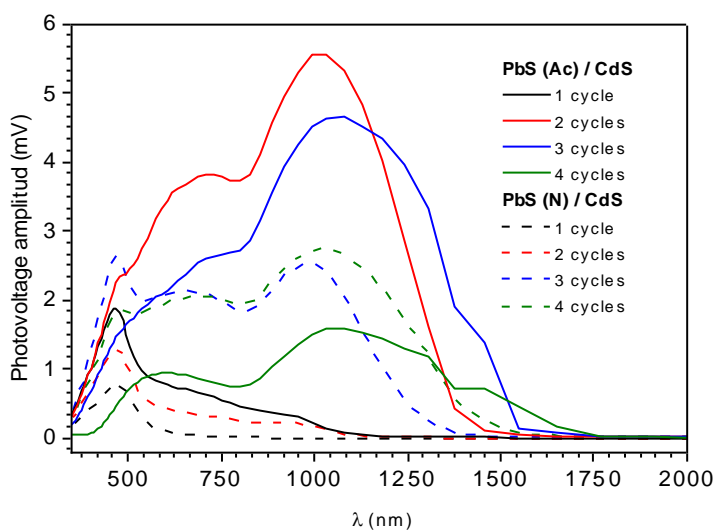
SI.4.- Dependence of cell performance on PbS SILAR cycles and lead precursor:

Photovoltaic performance depending on the number PbS SILAR cycles deposition and lead precursor.

Sample (PbS/CdS)	N° SILAR cycles (PbS/CdS)	J_{sc} (mA/cm ²)	V_{oc} (V)	FF	η (%)
(Ac)/(Ac)	1/5	18.04	0.481	0.489	4.24
	2/5	22.28	0.416	0.453	4.20
	3/5	14.19	0.348	0.433	2.14
	4/5	7.15	0.308	0.383	0.84
(N)/(Ac)	1/5	2.58	0.442	0.414	0.472
	2/5	13.37	0.481	0.490	3.16
	3/5	11.73	0.404	0.485	2.30
	4/5	9.90	0.391	0.434	1.68

SI.5.- SPV amplitude of PbS/CdS (Ac) samples in linear scale:

Fig. SI.5. Spectra of the surface photovoltage amplitude of PbS (Ac)/CdS (solid line) and PbS (N)/CdS (dashed line) samples for 1, 2, 3, and 4 cycles of PbS deposition by SILAR. 5 SILAR cycles with Cd (Ac) were used in all the cases for CdS growth.



SI.6.- Phase analysis of SPV characterization:

The SPV signal is proportional to the modulated density of charge separated in space and to the modulated distance of the centers of negative and positive charge.¹ Both depend sensitively on the dominating mechanisms of charge separation, recombination and local charge transport. Therefore the analysis of the phase angle allows to draw conclusions about changes of involved mechanisms of modulated charge separation. Fig. SP.6-1 shows the spectra of the phase angle of the surface photovoltage of PbS (Ac) / CdS (Ac) and PbS (N) / CdS (Ac) samples for 1, 2, 3, and 4 cycles of PbS deposition by SILAR. The phase angle changed over a wide range depending on the samples. For example, the phase angle was usually close to 90° for spectral range with charge separation from defect states.

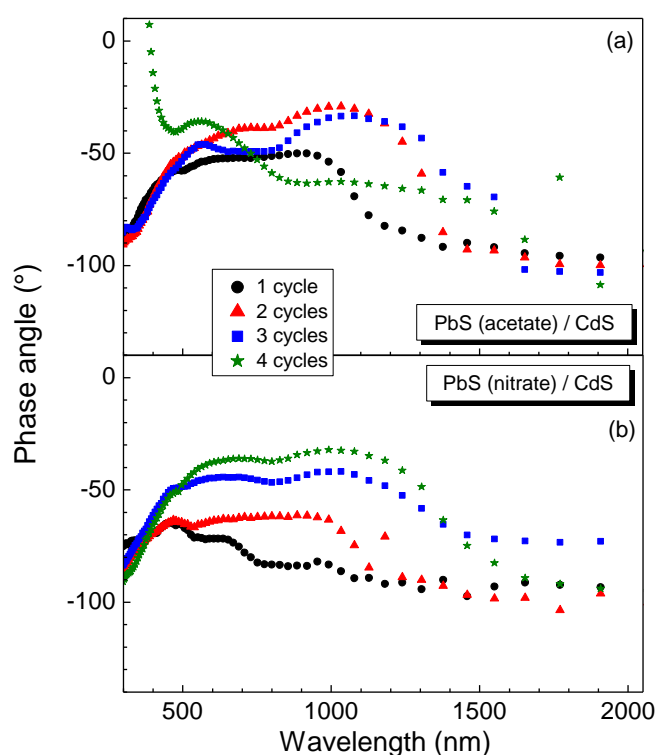


Fig. SI.6-1. Spectra of the phase angle of the surface photovoltage of (a) PbS (Ac) / CdS and (b) PbS (N) / CdS samples for 1, 2, 3, and 4 SILAR cycles of PbS deposition (circles, triangles, squares, and stars, respectively). 5 SILAR cycles and Cd (Ac) has been used as cadmium precursor in all the cases for CdS deposition.

For the PbS(Ac) samples the phase angle at 700 nm remained nearly constant (-52, -39, -49, and -46° for 1 SILAR cycle and 2, 3, and 4 SILAR cycles, respectively) whereas the phase angle decreased systematically for the PbS(N) samples with increasing number of SILAR cycles (-77, -63, -45 and -35° for 1 SILAR cycle and 2, 3, and 4 SILAR cycles, respectively). This behavior gives evidence for a relatively strong dependence of charge separation on the effective thickness of the PbS(N) layer. The

spectra of the phase angle show some similarity with the spectra of the SPV amplitude on logarithmic scale. This implements a certain dependence of the phase angle on the SPV amplitude. The phase angles are plotted as functions of the SPV amplitude of PbS(Ac) and PbS(N) samples for 1 SILAR cycle and 2, 3, and 4 SILAR cycles in figure Fig. SP.6-1.

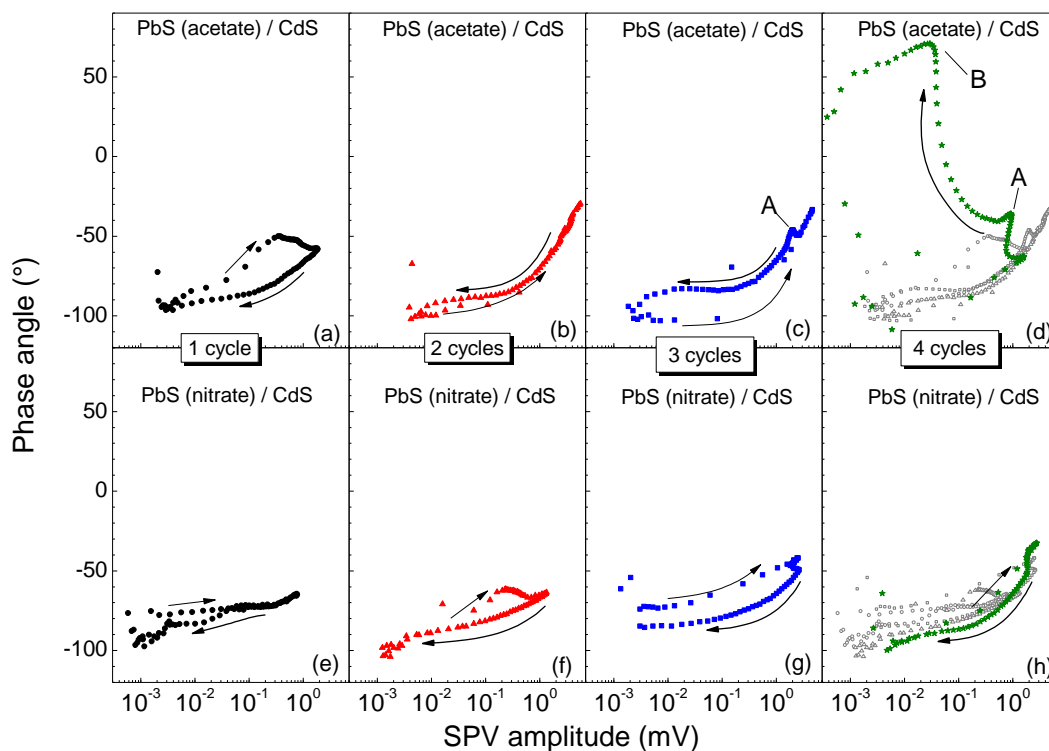


Fig. SI.6-2. Dependencies of the phase angle on the SPV amplitude of (a-d) PbS(Ac) and (e-h) PbS(N) samples for 1 SILAR cycle and 2, 3, and 4 SILAR cycles ((a,e), (b,f), (c,g) and (d,h), respectively). 5 SILAR cycles and Cd (Ac) has been used as cadmium precursor in all the cases for CdS deposition. The arrows mark the direction of decreasing wavelengths, A and B denote specific features.

The phase angles described practically one common dependence on the SPV amplitude for the PbS(Ac), 2 SILAR cycles sample with only a small hysteresis at low values of the SPV amplitude. Therefore, modulated charge separation of the PbS(Ac), 2 SILAR cycles sample is dominated by only one process. This process can be assigned to the modulated injection of electrons from PbS quantum dots into TiO₂ nanoparticles, their separation and recombination. In the dependence the phase angle decreased with increasing SPV amplitude, i.e. the relaxation of SPV signals became faster with increasing density of electrons in the sintered TiO₂ nanoparticles. This is not surprising if considering stationary filling of the deepest trap states in TiO₂ nanoparticles.

A hysteresis appeared in the dependence of the phase angle on the SPV amplitude for the PbS(Ac), 1 SILAR cycle sample. The hysteresis is caused by different mechanisms of charge separation in the near infrared and ultra-violet regions when defect states or states in CdS can play a dominant role, respectively. Since such a hysteresis did not appear in the PbS(Ac), 2 SILAR cycles sample it can be concluded that charge exchange between defect states at the external CdS surface and TiO₂ plays a significant role for modulated charge separation.

A hysteresis with opposite change of the phase angle and a small additional feature (denoted by A in Fig. SI.6-2(c)) were found for the PbS(Ac), 3 SILAR cycles sample in comparison to the PbS(acetate, 1 SILAR cycle) sample. The hysteresis is caused by charge separation from defect states at PbS quantum dots towards the internal interface, the additional feature gives evidence for an onset of charge separation within the PbS quantum dot layer. A change of the sign of the phase angle was discovered for the PbS(Ac), 4 SILAR cycles sample in the spectral range of strong light absorption (see feature denoted by B in Fig. SI.6-2(d). In this case electrons were separated predominantly towards the external surface of the CdS layer. Such behavior can be only explained if assuming a negatively charged interface layer between the PbS quantum dot and the CdS surface layer what is only possible if the conduction band edge of the TiO₂ nanoparticles as well as the conduction band edge of the CdS surface layer are above the states of excited electrons in the PbS quantum dots.

It has to be pointed out that, if excluding the hysteresis, all dependencies of the phase angle on the SPV amplitude were very similar for the PbS(Ac) samples, i.e. charge separation by injection of electrons from PbS quantum dots into TiO₂ nanoparticles and electron transport in TiO₂ nanoparticles dominated. Relatively strong hysteresis was always present and a rather common dependence were not found for the dependence of the phase angle on the SPV amplitude of the PbS(N) samples (compare Fig. SI.6-2(e-h)). This means that modulated charge separation was affected by several mechanisms while one of the mechanisms depended strongly on the effective thickness of the PbS quantum dot layer. We assume that uncontrolled side reactions during the SILAR process in the nitrate led to modifications of defect states.

As a conclusion, modulated charge separation in the TiO₂ / PbS quantum dot / CdS system can be dominated by only one mechanism if depositing the PbS by SILAR from an acetate solution.

References

1. I. Mora-Seró, T. Dittrich, G. Garcia-Belmonte and J. Bisquert, *Journal of Applied Physics*, 2006, **100**, 103705.